ADVANCED HEALTHCARE MATERIALS
www.advhealthmat.de

Dynamic Cellular Interactions with Extracellular Matrix Triggered by Biomechanical Tuning of Low-Rigidity, Supported Lipid Membranes

*Setareh Vafaei, Seyed R. Tabaei, Kabir H. Biswas, Jay T. Groves, and Nam-Joon Cho**

The behavior of cells in a tissue is regulated by chemical as well as physical signals arising from their microenvironment. While gel-based substrates have been widely used for mimicking a range of substrate rigidities, there is a need for the development of low rigidity substrates for mimicking the physical properties of soft tissues. In this study, the authors report the development of a supported lipid bilayer (SLB)-based low rigidity substrate for cell adhesion studies. SLBs are functionalized with either collagen I or fibronectin via covalent, amine coupling to a carboxyl group-modified lipid molecule. While the lipid molecules in the bilayer show long-range lateral mobility, the covalently functionalized extracellular matrix (ECM) proteins are immobile on the bilayer surface. Specific adhesion of cells results in an enrichment of the protein on the bilayer and the appearance of a zone of depletion around the cells. Further, the lateral reorganization of the ECM proteins is controlled by altering the fluidity of lipid molecules in the substrate. Thus, the experimental platform developed in this study can be utilized for addressing basic questions related to cell adhesion on low rigidity substrates as well as biomedical applications requiring adhesion of cells to low rigidity substrates.

1. Introduction

With growing evidence that mechanical[1] and geometrical[2] factors play key roles in regulating cellular responses within tissue microenvironments, there are extensive efforts to design biomimetic platforms that mimic natural tissue interfaces and provide a guiding force to engineer cell behavior. In general, this natural sensitivity to physical microenvironmental signals presents a difficulty for in vitro cellular studies, in which cells are cultured on synthetic substrates. Conventional plastic cell culture plates present an extremely stiff substrate, at the far end of the spectrum of mechanical stiffness experienced by cells in physiological settings.[3] Polydimethyl siloxane (PDMS) and other polymeric substrates have been used to access softer regimes, yielding many important insights into the role of mechanical properties of the microenvironment in cellular behavior.[3,4] However, these polymer gel substrates still have difficulty accessing the softest and most fluid interfaces that cells may experience in a physiological environment.

Supported lipid membranes, consisting of continuous phospholipid bilayers assembled on a solid substrate, have proven useful in a wide variety of cellular and biomolecular studies.[2b,c,5] The supported membrane presents a naturally fluid surface, with lipids and membrane-associated proteins free to diffuse within the membrane. Typical 2D lateral diffusion coefficients in low-defect supported membranes are in the range of a few $\mu m^2\ s^{-1}$. As such, supported membranes present a relatively viscous, but not elastic environment that resembles the natural cell membrane. Thus, the fluid nature of supported membranes is useful to access the extremely low stiffness end of the mechanical spectrum that cells may experience in a physiological environment.

2. Results and Discussion

To generate a low rigidity substrate for integrin-mediated cell adhesion, we functionalized extracellular matrix (ECM) proteins on fluid supported lipid bilayers (SLBs). **Figure 1**a provides a schematic illustration of an SLB platform decorated with ECM. Briefly, SLBs composed of a zwitterionic lipid (1,2-dioleoyl-sn-glycero-3-phosphatidylcholine, DOPC) and varying fraction (up to 20%) of a lipid with a free carboxylic acid (1,2-dipalmitoyl-sn-glycero-3-phosphoethanolamine-*N*-(glutaryl),DP-NGPE),

S. Vafaei, Dr. S. R. Tabaei, Prof. N.-J. Cho
Centre for Biomimetic Sensor Science
Nanyang Technological University
50 Nanyang Drive 637553, Singapore, Singapore
E-mail: njcho@ntu.edu.sg
S. Vafaei, Dr. S. R. Tabaei, Prof. N.-J. Cho
School of Materials Science and Engineering
Nanyang Technological University
50 Nanyang Avenue 639798, Singapore, Singapore
Dr. K. H. Biswas, Prof. J. T. Groves
Mechanobiology Institute
National University of Singapore
117411, Singapore, Singapore
Prof. J. T. Groves
Department of Chemistry
University of California
Berkeley, CA 94720, USA
Prof. N.-J. Cho
School of Chemical and Biomedical Engineering
Nanyang Technological University
62 Nanyang Drive 637459, Singapore, Singapore

DOI: 10.1002/adhm.201700243

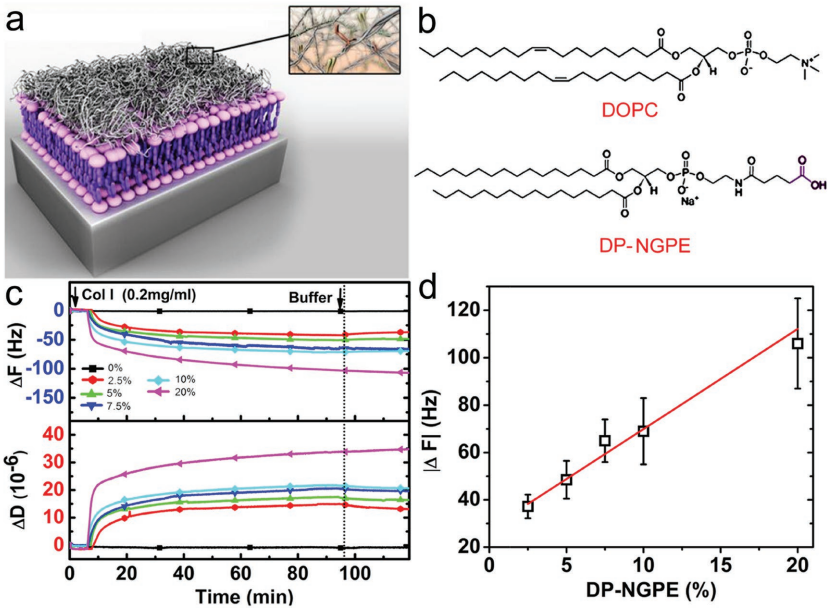

Figure 1. Characterization of ECM-functionalized supported lipid bilayer (SLB). a) Schematic illustration of collagen type I (Col I) bound to SLB via amine coupling. b) Structures of the lipids used in this study, together with their chemical names. c) The QCM-D frequency (ΔF) and dissipation (ΔD) change after Col I binding to DOPC bilayers prepared by SALB method using varying mole fractions of functional lipid bearing a free carboxylic acid for amine coupling (DP-NGPE) in the lipid precursor mixture (between 0 and 20 mol%). After bilayer fabrication, the frequency shift was then normalized with $\Delta F = 0$ Hz corresponding to the planar lipid bilayer in each experiment. Changes in resonance frequency indicate the adsorption of Col I onto the bilayers. d) The absolute frequency shift ($|\Delta F|$) upon Col I binding onto bilayer versus mole fraction of DP-NGPE included in the precursor mixture.

(Figure 1b) were deposited on glass coverslips using the recently developed solvent assisted lipid bilayer (SALB) formation method that is highly flexible with the nature of the constituent lipids.[6] ECM proteins were functionalized covalently to lipid molecules present on bilayers via amine coupling, similar to a previously described strategy.[7] Bilayers composed of a zwitterionic lipid (DOPC) and varying fraction (up to 20%) of a lipid with a free carboxylic acid (DP-NGPE) were formed on SiO_2 substrates using SALB formation method (Figure S1, Supporting Information). Post assembly of lipid bilayers, the carboxylic acid group on DP-NGPE was activated via the 1-ethyl-3-(3-dimethylaminopropyl)carbodiimide/*N*-hydroxysuccinimide (EDC/NHS) chemistry. Following the activation of the carboxylic group, ECM proteins were added to allow covalent coupling of the proteins to the bilayer.

A key consideration in using the present method for bilayer formation is that not all lipid molecules are equally favored for incorporation into the bilayer. It is likely that anionic lipids such as the one used here, i.e., DP-NGPE will be less favorably incorporated into the bilayer that are assembled on a negatively charged SiO_2 substrate.[8] Therefore, a range of mole fractions of the functional lipid was used to form SLBs to assess the functionalization of ECM proteins. Figure 1c presents the changes in the quartz crystal microbalance with dissipation (QCM-D) frequency (ΔF) and energy dissipation (ΔD) upon addition of collagen type I solution (Col I) to bilayers prepared by including different fractions of DP-NGPE in their precursor lipid mixture. The ΔF and ΔD are related to the mass and the viscoelastic properties (rigidity and softness) of the adlayer, respectively. A negative shift in ΔF indicates increase in the mass due to protein adsorption. Addition of Col I to pure DOPC bilayer resulted in almost no change in QCM-D frequency and dissipation. This is expected as zwitterionic lipid bilayers resist protein adsorption in general, and has been utilized as antifouling surfaces. However, a negative ΔF was observed for bilayers containing the functional lipid (DP-NGPE) suggesting specific adsorption of Col I to the bilayer. Addition of Col I to bilayer prepared using 20 mol% DP-NGP with and without NHS activation step resulted in a negative frequency shifts of -126 ± 8 Hz and 11.3 ± 2.1 Hz, respectively suggesting that majority of proteins specifically attached to the activated free carboxylic acid group of the functional lipid (DP-NGPE).

Figure 1d shows that the QCM-D frequency shift upon Col I binding to functionalized SLBs depends linearly on the fraction of functional lipids included in the original lipid mixture. This is despite the fact that the adlayer is not completely rigid, as assessed from the high energy dissipation, which may suggest that the relationship between frequency shift and the actual adsorbed mass may not be linear. Nevertheless, the linear dependence suggests that the amount of Col I covalently coupled can be modulated by the fraction of functional lipids included in the precursor lipid mixture. In addition, the high-energy dissipation observed here indicates the softness of the protein-lipid adlayer, suggesting that the Col I fibers attached to the SLB are not rigid. About 3% of the total amino acids in Col I is lysine and thus, a limited number of sites of covalent coupling on the fibers allow them to retain their flexibility while attached to the bilayer.

Immunofluorescence imaging of the Col I functionalized bilayer showed randomly oriented fibers on the membrane surface (Figure S2, Supporting Information). Consistent with the QCM-D results, the density of Col I fibers adsorbed to the bilayer increased with the fraction of functional lipids in the original lipid mixture. However, a more homogeneous distribution of Col I was observed when above 10 mol% DP-NGPE functional lipid was used. Therefore, we conducted the rest of experiments using bilayers prepared by including 20 mol% DP-NGPE in the lipid precursor mixture. Next we evaluated the attachment of cells to bilayers prepared using different fraction DP-NGPE (Figure S3, Supporting Information). Indeed the number of attached cells increased with increasing fraction of DP-NGPE in the bilayer and thus with increasing density of proteins. These results indicate that in this protein regime, the protein density regulates the efficiency of cell attachment.

A requirement for full-filling the criteria of a low rigidity substrate, is that the lipid molecules are diffusive after functionalization of the ECM proteins. In order to determine if

the bilayers functionalized with Col I exhibit long-range lateral diffusion, a microscope-based fluorescence recovery after photobleaching (FRAP) experiment was performed on the bilayers. The fluorescent 1,2-dioleoyl-sn-glycero-3-phosphoethanolamine-*N*-(lissamine rhodamineB sulfonyl)(ammonium salt) (Rh-PE) lipid was included in the bilayer for this. In Figure S4 in the Supporting Information, left and right panels show fluorescence micrographs of the bilayer (20% DP-NGPE) at $t = 0$ and 60 s after photobleaching, respectively, revealing a near-complete recovery of the fluorescence at the photobleached spot. While the lipid diffusion coefficient on ECM protein functionalized bilayer was found to be slightly lower than the nonfunctionalized bilayer, a bilayer with a diffusion coefficient of $2.0 \pm 0.1\ \mu m^2\ s^{-1}$ is sufficiently fluid to be used as extremely low rigidity substrates.

We followed essentially the same approach for preparing SLB substrates functionalized with fibronectin (FN) (Figure S5a,b, Supporting Information). In agreement with the QCM-D data, immunofluorescence microscopy of the FN functionalized SLBs showed increased protein densities with increasing fraction of functional lipids (Figure S6, Supporting Information). The fluorescence micrographs also show the presence of some unevenly distributed FN, which appeared as particularly brighter spots. This is in agreement with a previous atomic force microscopy-based study of the interaction of FN with supported bilayer, which revealed the formation of FN aggregate at the membrane interface.[9] FRAP analysis of FN functionalized bilayer, showed that the membrane retains its long-range lateral mobility, albeit with a reduced diffusivity ($D = 1.4 \pm 0.1\ \mu m^2\ s^{-1}$).

Having observed the long-range, lateral diffusion of lipid molecules in the bilayer, we attempted to determine the diffusion behavior of the covalently bound proteins on the bilayer. Protein diffusion on a membrane is thought to be primarily governed by the diffusive properties of the lipid molecules.[10] However, fluorescence imaging showed that FN and Col I fibers practically were immobile in the time scale of experiments (3 h). This perhaps reflects the fact that individual ECM proteins are covalently bound to multiple lipid molecules, and hence, displays a reduced diffusion.[11] Such an idea is supported by the observed reduction in the diffusion coefficient of lipid molecules on ECM protein functionalized bilayers (2.0 ± 0.1 and $1.4 \pm 0.1\ \mu m^2\ s^{-1}$ for Col I and FN functionalized bilayers, respectively, versus $2.4 \pm 0.1\ \mu m^2\ s^{-1}$ for nonfunctionalized bilayers). However, unlike the display of highly diffusive proteins on bilayers,[2b,c,12] this display of immobile proteins on fluid bilayers is better suited for cell adhesion studies that require a reduction in the diffusion of the protein.[5e,f] More specifically, this immobile display of ECM proteins on fluid bilayer appears to be a better mimic of low rigidity matrices that also display immobilized proteins.[3,4b,d]

Having established an ECM protein functionalized bilayer substrates, we chose the hepatocyte cancer cell line, Huh 7.5, which has been previously utilized for studies related to the effect of ECM proteins on hepatocyte cell behavior and differentiation.[13] Cells were plated on both the Col I and FN-functionalized bilayers, and their interaction with ECM proteins were monitored by fluorescence as well as reflectance interference contrast microscopy (RICM)[14] (Figure S7, Supporting Information). Fluorescence microscopy enables visualization of changes in the integrity and distribution of fluorescently-labeled ECM proteins during their interaction with individual cells. Cell adhesion and spreading depend strongly on the interaction between cell and ECM molecules. Huh 7.5 cells readily attached to Col I-functionalized bilayer (**Figure 2**a). In contrast, almost no attachment was observed for cells plated onto nonfunctionalized bilayers, consistent with previous observations,[15] suggesting that the functionalization of the bilayer with Col I resulted in the specific adhesion of the cells.

Importantly, we found that the interaction of the cells with the bilayer resulted in a local enrichment of the fluorescently-labeled Col I underneath cell while a zone of depletion was observed around the cell after 3 h (Figure 2a). This observation was specific to Col I-functionalized bilayer since neither enrichment nor depletion of the fluorescently-labeled Col I was observed on glass surfaces, even though the cells showed robust adhesion on such surfaces (Figure 2b). Importantly, RICM imaging of the adhering cells showed a close association of the adhering cells with both types of surfaces (Figure 2g). Additionally, adhering cells showed reduced contact area and polarization (as assessed by the circularity of the cell adhesion zone)[3b] on Col I-functionalized bilayers in comparison to Col I-functionalized glass surfaces (Figure 2h,i). Similar results were obtained in experiments with FN (Figure 2c,d,g,h,i). These results suggest that application of forces by the adhering cells on the bilayer-bound Col I molecules causes a lateral movement of the molecule that eventually results in an enrichment of the protein underneath the cell. However, such forces are probably not sufficient to cause dislocation of the protein that are adsorb on glass surfaces. As we have mentioned in the introduction part of the manuscript, SLBs are viscous but not elastic, and thus application of cellular forces on ECM proteins will lead to their dislocation in the lateral dimension. However, given the viscous nature of SLBs, the lateral translocation of the ECM proteins will result in the development of a viscous drag force. Such a force has been estimated using the Einstein–Smoluchowski relation on SLBs functionalized with cadherin adhesion protein and was found to be in the range of femtoNewtons (fN),[5e] which are much lower than the few to tens of picoN reported for integrin-ECM interaction on stiff substrates.[16]

The local depletion of the ECM proteins observed here appears to be similar to previous results obtained with nanoparticle coated solid surfaces.[17] While these local depletion of the ECM proteins appear to be similar to the engulfment of nanocrystals reported previously (citations), these two systems are fundamentally different in that the ECM proteins are covalently linked to the supported lipid bilayer while the nanocrystals adhere to the collagen coated glass surface in a nonspecific manner.

A lateral translocation of the Col I molecules underneath adhering cells will require that the bilayer retains its long-range lateral mobility after the cell adhesion. Therefore, we performed FRAP experiments at the zone of cell adhesion to assess the mobility of lipid molecules (Figure 2e,f). FRAP experiments revealed a diffusion coefficient of 1.99 ± 0.06 and $1.4 \pm 0.05\ \mu m^2\ s^{-1}$ for Col I and FN-functionalized bilayers, respectively, confirming that the bilayers still retain their fluidity. The slight reduction in the diffusion coefficient observed under adhering cells is likely due to the greater accumulation

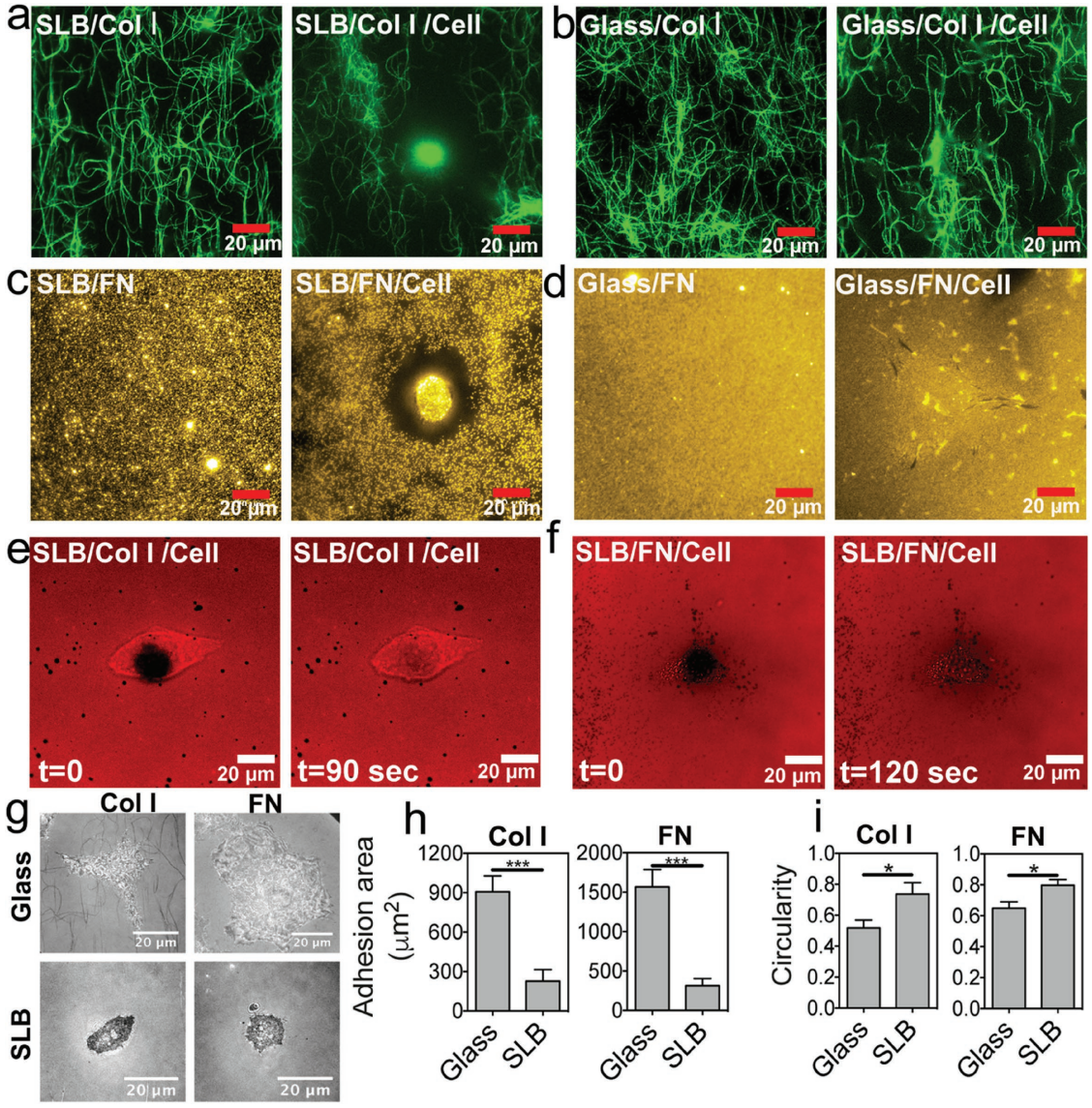

Figure 2. Cell behavior on ECM-coated bilayer and glass surfaces. a) Representative fluorescence image of stained collagen fibers on SLB before (left) and 3 h after plating (right) of the hepatocyte cells (Huh 7.5). Col I fibers around the cell were depleted by the cell following adhesion and spreading. b) Fluorescence micrograph of an adherent cell 3 h after cell attachment on Col I coated glass showed no collagen depletion. Representative fluorescence image of FN coated bilayer, before and 3 h after cell adhesion demonstrating fibronectin depletion. Fibronectin depletion by cell was not observed on (d) fibronectin coated glass. FRAP snapshots of supported bilayer underneath the cell plated on e) Col I and f) FN coated bilayer after 3 h after cell adhesion. Fluorescence was recovered nearly completely suggesting bilayer retains its mobility underneath the cell. g) RICM images of cells adhering Col I and FN-functionalized glass and bilayer substrates. Note the greater spread of the cells on the glass substrate compared to the bilayer substrate. Graph showing h) adhesion area (contact) and i) circularity of cells on different substrates. Note that lower cell adhesion area and higher circularity of cells on bilayer substrates. Error bars are s.e.m. of measurements made from ≈10 cells in each group. * indicates p value less than 0.05 while *** indicates p value less than 0.001.

of the lipid molecules that are covalently bound to the ECM proteins. This confirms that the enrichment of Col I and FN observed on bilayers is enabled by the lateral mobility of the lipid molecules.

After establishing a low rigidity substrate for cell adhesion, we manipulated the bilayer viscosity to determine its role in the cell adhesion and enrichment of ECM proteins. Membrane viscosity directly controls the tension developed upon the application of cellular forces on the covalently bound ECM proteins.[5e] We altered the viscosity of the bilayers by adding cholesterol (Chol) in the bilayers. Controlling cholesterol content in the plasma membrane of cells have been previously utilized to regulate their membrane viscosity,[18] which in turn regulate the dynamics of membrane proteins[19] and the rate of cell migration.[20] We chose the SALB method of bilayer formation for this as it has been already shown to allow assembly of bilayers with a high cholesterol content.[21] Bilayers were prepared with a range of cholesterol fraction (up to 40%), and functional-

ized with either Col I or FN as described in the previous section. The protein adsorption level to cholesterol-containing bilayers was almost the same as that of bilayers with no cholesterol (Figure S8, Supporting Information). It is expected as cholesterol only affects the viscosity of the membrane while the protein adsorption is mainly determined by the fraction of activated functional lipids present in the membrane.

Diffusion coefficients of lipids were determined by FRAP, and membrane viscosity was estimated from the diffusion coefficients by applying the Evans–Sackman model[22] (see the Experimental Section for details). **Figure 3**a,b shows the diffusivity and membrane viscosity of nonfunctionalized and ECM protein-functionalized bilayers with varying fraction of cholesterol, respectively. Generally, the diffusivity of lipids decreased with increased fraction of cholesterol. For instance, the lipid diffusivity of nonfunctionalized membranes was reduced almost four times from 2.3 ± 0.3 to 0.6 ± 0.2 μm^2 s^{-1}, when 40% cholesterol was included in the bilayer (Figure 3a). Accordingly, the membrane viscosity was increased almost six times from $6.7 \pm 1.1 \times 10^{-10}$ to $37.4 \pm 4.5 \times 10^{-10}$ kg s^{-1}. Importantly, while the lipid diffusion coefficients at low cholesterol fractions (≤10%) were different between the nonfunctionalized and ECM protein functionalized bilayers (Figure 3a), they were similar at higher cholesterol fractions indicating a dominating effect of cholesterol on bilayer diffusivity in comparison to the effect of covalent coupling of the ECM proteins to the bilayer.

Increasing the fraction of cholesterol in the bilayer resulted in a reduction in the amount of Col I depletion by adhering cells. The areas of depletion zones around cells that were cleared of fluorescently labeled protein and the areas of the

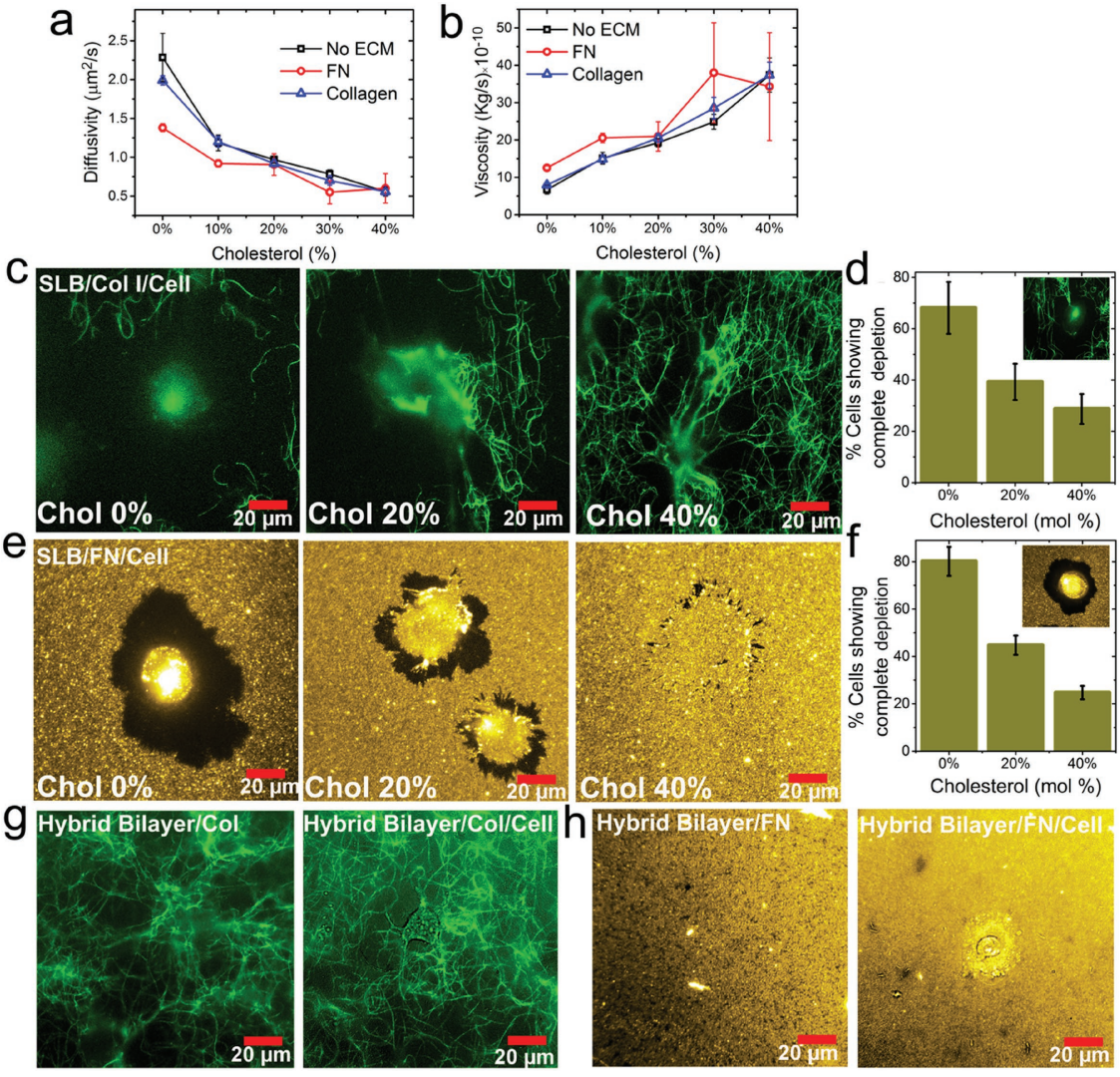

Figure 3. Effect of membrane viscosity on cell behavior plated on ECM-functionalized bilayer platforms. a) Membrane diffusivity and b) the corresponding viscosity of bare and ECM-functionalized SLBs (20% DP-NGPE), containing varying fraction of cholesterol. Fluorescence micrograph of c) Col I and e) FN on supported bilayer with varying fraction of Chol (0%, 20%, and 40%) incubated with Huh 7.5 for 3 h. With increasing the percentages of Chol, the protein depletion decreased. Percentage of cells showing complete protein depletion on d) Col I and f) FN functionalized bilayers with varying fraction of cholesterol. Fluorescence micrographs of g) Col I and h) FN on hybrid bilayers before and after incubation with Huh 7.5 for 3 h. No depletion was observed on hybrid bilayers.

corresponding cells were determined using ImageJ software. We assigned cases which the area of the depletion zone was greater than the area of the corresponding cell to the complete depletion group (Figure S9, Supporting Information). The majority (68 ± 10%) of cells on bilayers with no cholesterol showed complete Col I depletion (see Figure 3d, inset), however, only 39 ± 7 and 28 ± 5% of cells on bilayer containing 20% and 40% cholesterol respectively, showed complete depletion. The rest of the cells in these samples showed partial or no depletion (see Figure 3c). A similar trend was observed for cells on FN-functionalized bilayers (Figure 3e,f). These results suggest that increasing the viscosity of the bilayer results in a decrease in the later translocation of the ECM proteins on the bilayer.

The reduction in the lateral translocation of the ECM proteins on 40% cholesterol-containing bilayers was interesting. Although cholesterol lead to a reduction in the fluidity of the bilayer, it is not clear if the effects seen with cells were entirely due to the increase in the viscosity, and is not due to any chemical effects of cholesterol. To confirm that the effects seen with cells are purely due to the change in the physical properties of the substrate, we prepared hybrid substrates composed of a phospholipid monolayer on top of a hydrophobic alkane-silane self-assembled monolayer on glass using the SALB method.[6] The lipid mobility in these substrates was very slow, and a FRAP analysis revealed a diffusivity of $0.2 \pm 0.04\ \mu m^2\ s^{-1}$, which is in the range previously reported values,[23] and corresponds to a viscosity of $123 \pm 30 \times 10^{-10}$ kg s^{-1}. Col I and FN were readily conjugated to the hybrid bilayers containing 20% functional lipids, as judged from fluorescence imaging (Figure 3g,h). Similar to the results obtained with high cholesterol-containing bilayers, less than 10% of cells showed a depletion of either Col I or FN on these substrates. This confirms that the reduction in the fraction of cells showing lateral movement of ECM proteins is controlled by the viscosity of the underlying bilayer.

3. Conclusion

In conclusion, we have developed a bilayer-based low-rigidity substrate displaying ECM proteins through covalent coupling that allows cell adhesion. Cells adhering to these substrates show lateral translocation of the ECM protein resulting in the formation of a zone of enrichment of ECM proteins underneath them, and a zone of depletion of ECM proteins around them. This lateral translocation is enabled by the long-range diffusivity of the underlying supported lipid bilayer, and can be controlled by altering the diffusivity of the bilayer. Given the lateral translocation of the ECM proteins, it appears that these substrates provide a range of substrate rigidity that is probably not achievable by currently used PDMS-based substrates. We envisage that the low-rigidity substrate developed here will be useful in enabling both the short-term (within hours) adhesion, and long-term (within days) gene expression changes and differentiation of stem cells. In addition, these substrates will be useful in biomedical applications requiring cell adhesion to extremely low-rigidity surfaces such as in the case of neuronal tissues.

4. Experimental Section

Lipid Sample Preparation: DOPC, DP-NGPE, Chol, and fluorescently labeled lipid, Rh-PE were purchased form Avanti Polar Lipid (Alabaster, AL). The powders were dissolved in isopropanol at a nominal concentration of 10, 25, and 1 mg mL^{-1}, respectively. Due to the insolubility of DP-NGPE in isopropanol, the powder was dissolved in ethanol (99.99%) at 5 mg mL^{-1} lipid concentration and was heated to 50 °C and gently vortexed. The stock solutions were diluted in isopropanol to the desired DOPC:DP-NGPE:Cho molar ratios, and then diluted to 0.5 mg mL^{-1} lipid concentration. In fluorescence microscopy experiments, 0.5 wt% Rh-PE was included in the lipid composition.

QCM-D: A Q-Sense E4 instrument (Q-sense AB, Gothenburg, Sweden) was used to monitor the kinetics of lipid bilayer formation and subsequent protein adsorption on SiO_2 coated 5 MHz, AT-cut piezoelectric quartz crystal. Temporal changes in frequency and dissipation were recorded as previously described.[24] All the QCM-D measurements were recorded at 3, 5, 7, and 11 overtones at 24.00 ± 0.5 °C. A peristaltic pump (Ismatec Reglo Digital) was used to introduce sample into the measurement chamber at 50 µL min^{-1}.

Substrate Preparation: Two different substrates including silicon oxide (SiO_2) coated QCM-D crystal chips (Q-sense AB, Gothenburg, Sweden) and glass were submerged in 1% sodium dodecyl sulfate and rinsed with Milli-Q water (Millipore) extensively. After drying the substrates with nitrogen gas, SiO_2 and glass were treated with oxygen plasma (March Plasmod Plasma Etcher, March Instruments, California) at about 180 W for 1 min and 5 min, respectively.

Silanization of Glass Substrates: Glass was silanized in a 1 vol% solution of Octa-decyl-tri-chloro-silane (Sigma) in dry toluene (Merck) at room temperature for 1 h. Silanized substrates were finally rinsed with toluene, methanol (Merck), and Milli-Q water.

Lipid Bilayer Formation: The SALB method was utilized to form lipid bilayer. In brief, lipids in a mixture of isopropanol were incubated with the substrate for 10 min. After lipid deposition, the organic solvent was gradually exchanged by aqueous buffer (10×10^{-3} M Tris + 100×10^{-3} M NaCl, pH 7.2). In case of bilayer formation on glass-based surface, commercially available microfluidic flow cells (stick-Slide, ibidi) were utilized. The rate of injection flow was 50 µL min^{-1}.

Activation of Carboxylic Group of DP-NGPE Lipid Included-Supported Lipid Bilayer by EDC/NHS Treatment: For Conjugating protein with SLB, DP-NGPE as a functionalized lipid was activated by a solution of 10 mg mL^{-1} *N*-hydroxysulfosuccinimide sodium (sNHS)/1-(3-Dimethylaminopropyl)-3-ethylcarbodiimide hydrochloride (EDC) (VWR) in pH 5.5 HEPES (10×10^{-3} HEPES +100×10^{-3} NaCl) immediately before used. The solution was incubated with SLB for 1 h to convert carboxylic groups to amine-reactive NHS ester.

Protein Sample Preparation and Adsorption on SLB and Glass: Protein samples were prepared in pH 7.5 phosphate-buffered saline (10×10^{-3} PBS, 2.7×10^{-3} KCL, and 150×10^{-3} NaCl) as a following concentrations: 0.2 mg mL^{-1} Col I (Sigma-Aldrich), 0.2 mg mL^{-1} FN (Calbiochem). Protein solutions were introduced on SLB and incubated for about 2 h to form Col I-SLB or FN-SLB. Finally the substrates were washed with PBS to remove unbounded proteins. As a control experiment, a similar process was performed to form single and multiple protein samples on glass/SiO_2 substrates.

FRAP and RICM: To do FRAP experiment, a 532 nm, 100 mW laser beam was applied to photobleach fluorescent lipid (Rh-PE) embedded in the bilayer in a specific area (small spot). The duration of photobleaching was around 5 s and the wideness of the black spot was 20 µm. All the fluorescence image and videos presented in this paper were captured using an inverted epifluorescence Eclipse TE 2000 microscope (Nikon) equipped with a 10×/60× oil immersion objective (NA 1.49), and an Andor iXon + Evolve electron multiplying charge-coupled device (EMCCD) camera (Andor Technology, Belfast, Northern Ireland). The acquired images had dimensions of 512 × 512 pixels with a pixel size of 0.267 × 0.267 µm. The recovery was followed

at 2 s intervals, and diffusion coefficients were computed using the Hankel transform method 2. RICM imaging was performed using an Eclipse Ti inverted microscope (Nikon) equipped with an EMCCD camera (Photo- metrics) while images were collected using Metamorph (Molecular Devices). All image processing was done using ImageJ software.

Estimation of Membrane Viscosity: The viscosity of the supported bilayer was calculated using the Evans–Sackmann model for cylindrical particles embedded within a solid supported, fluidic membrane[22a]

$$D = \frac{k_B T}{4\pi\eta_M}\left(\frac{1}{2}\varepsilon^2 + \frac{\varepsilon K_1(\varepsilon)}{K_0(\varepsilon)}\right)^{-1} \quad (1)$$

where $\varepsilon = a_C\sqrt{\frac{b}{\eta_M}}$

In Equation (1), D is the diffusivity of lipids measured using FRAP, a_C is the radius of a single lipid molecule (0.45 nm),[25] η_M is the monolayer (half the bilayer) viscosities, K_0 and K_1 are the zeroth and first order modified Bessel functions of the second kind, and $b = 2 \times 10^7$ kg s^{-1} m^{-2},[26] is a phenomenological friction coefficient, to account for the presence of the solid support.

Cell Culture: Human hepatocarcinoma cell line (Huh-7.5; Apath) was used as a hepatocyte model in this study. The cells were grown on 100 mm tissue culture plates in supplemented growth media containing Dulbecco's modified eagle's medium (Hyclone), 10% fetal bovine serum (Hyclone) and 1% penicillin and streptomycin (Gibco). The media was changed every 3 d. When the confluence of the cells reached about 70%, 0.25% trypsin (Gibco) was used for 3 min to separate Huh 7.5 cells from the tissue culture plates. Cell numbers were counted using hemocytometer and 1×10^3 Huh 7.5 cells were seeded on with and without proteins-functionalized SLB. As a control experiment, bare glass and protein-functionalized glass were used to compare with SLB-based surfaces.

Immunofluorescent Stain for ECM Proteins: To study ECM protein conformation and their interactions with Huh 7.5, Col I and FN was stained using primary and fluorescent labeled secondary antibody. In brief, before cell seeding, conjugated Col I and FN were washed with PBS three times to remove all unbounded proteins. Next, primary antibody for Col I: mouse monoclonal anti-Col I (abcam) and FN: mouse monoclonal IgG1 anti-FN (Santa Cruz, USA) was added in the samples with a volumetric dilution of 1:1000 and 1:50 in PBS respectively. After incubation for 2 h at room temperature, the samples were washed with PBS properly. Secondary antibodies including, Alexa Fluor 488 Goat Anti-mouse IgG (H + L) (LifeTechnology) and Alexa Fluor 555 Rabbit Anti-Mouse IgG (H + L) (LifeTechnology) were diluted in PBS (1:3000) and incubated with the Col I and FN for 15 min, respectively. Finally, the samples were washed with PBS and covered with aluminum foil for light protection. The images were captured using an inverted epifluorescence Eclipse TE 2000 microscope (Nikon) equipped with a 10×/60× oil immersion objective (NA 1.49), and an Andor iXon+ EMCCD camera (Andor Technology, Belfast, Northern Ireland). All image processing was done using ImageJ software.

Supporting Information

Supporting Information is available from the Wiley Online Library or from the author.

Acknowledgements

The authors would like to acknowledge the support from National Research Foundation (NRF-NRFF2011-01) to N.-J. Cho.

Keywords

cell adhesion, extracellular matrix, membrane viscosity, supported lipid bilayer

Received: February 23, 2017
Published online: March 30, 2017

[1] a) D. E. Discher, P. Janmey, Y. L. Wang, *Science* **2005**, *310*, 1139; b) M. J. Dalby, N. Gadegaard, R. Tare, A. Andar, M. O. Riehle, P. Herzyk, C. D. Wilkinson, R. O. Oreffo, *Nat. Mater.* **2007**, *6*, 997; c) D. T. Butcher, T. Alliston, V. M. Weaver, *Nat. Rev. Cancer* **2009**, *9*, 108; d) P. Tseng, D. Di Carlo, *Adv. Mater.* **2014**, *26*, 1242.

[2] a) C. M. Nelson, M. M. Vanduijn, J. L. Inman, D. A. Fletcher, M. J. Bissell, *Science* **2006**, *314*, 298; b) K. D. Mossman, G. Campi, J. T. Groves, M. L. Dustin, *Science* **2005**, *310*, 1191; c) K. Salaita, P. M. Nair, R. S. Petit, R. M. Neve, D. Das, J. W. Gray, J. T. Groves, *Science* **2010**, *327*, 1380.

[3] a) A. J. Engler, S. Sen, H. L. Sweeney, D. E. Discher, *Cell* **2006**, *126*, 677; b) M. Prager-Khoutorsky, A. Lichtenstein, R. Krishnan, K. Rajendran, A. Mayo, Z. Kam, B. Geiger, A. D. Bershadsky, *Nat. Cell Biol.* **2011**, *13*, 1457.

[4] a) S. V. Plotnikov, A. M. Pasapera, B. Sabass, C. M. Waterman, *Cell* **2012**, *151*, 1513; b) D. Choquet, D. P. Felsenfeld, M. P. Sheetz, *Cell* **1997**, *88*, 39; c) G. Giannone, B. J. Dubin-Thaler, H. G. Dobereiner, N. Kieffer, A. R. Bresnick, M. P. Sheetz, *Cell* **2004**, *116*, 431; d) T. A. Ulrich, E. M. de Juan Pardo, S. Kumar, *Cancer Res.* **2009**, *69*, 4167.

[5] a) A. Grakoui, S. K. Bromley, C. Sumen, M. M. Davis, A. S. Shaw, P. M. Allen, M. L. Dustin, *Science* **1999**, *285*, 221; b) E. Natkanski, W. Y. Lee, B. Mistry, A. Casal, J. E. Molloy, P. Tolar, *Science* **2013**, *340*, 1587; c) S. J. Fleire, J. P. Goldman, Y. R. Carrasco, M. Weber, D. Bray, F. D. Batista, *Science* **2006**, *312*, 738; d) A. C. Greene, S. J. Lord, A. Tian, C. Rhodes, H. Kai, J. T. Groves, *Biophys J* **2014**, *106*, 2196; e) K. H. Biswas, K. L. Hartman, C.-h. Yu, O. J. Harrison, H. Song, A. W. Smith, W. Y. Huang, W.-C. Lin, Z. Guo, A. Padmanabhan, *Proc. Natl. Acad. Sci. USA* **2015**, *112*, 10932; f) K. H. Biswas, K. L. Hartman, R. Zaidel-Bar, J. T. Groves, *Biophys. J.* **2016**, *111*, 1044; g) J. van Weerd, M. Karperien, P. Jonkheijm, *Adv. Healthcare Mater.* **2015**, *4*, 2743; h) D. H. Kim, H. Lee, Y. K. Lee, J. M. Nam, A. Levchenko, *Adv. Mater.* **2010**, *22*, 4551.

[6] a) S. R. Tabaei, J.-H. Choi, G. Haw Zan, V. P. Zhdanov, N.-J. Cho, *Langmuir* **2014**, *30*, 10363; b) S. R. Tabaei, J. A. Jackman, S.-O. Kim, V. P. Zhdanov, N.-J. Cho, *Langmuir* **2015**, *31*, 3125.

[7] C. J. Huang, N. J. Cho, C. J. Hsu, P. Y. Tseng, C. W. Frank, Y. C. Chang, *Biomacromolecules* **2010**, *11*, 1231.

[8] S. R. Tabaei, S. Vafaei, N.-J. Cho, *Phys. Chem. Chem. Phys.* **2015**, *17*, 11546.

[9] D. Nordin, O. Yarkoni, N. Savinykh, L. Donlon, D. Frankel, *Soft Matter* **2011**, *7*, 10666.

[10] P. Saffman, M. Delbrück, *Proc. Natl. Acad. Sci. USA* **1975**, *72*, 3111.

[11] a) Y. Gambin, R. Lopez-Esparza, M. Reffay, E. Sierecki, N. Gov, M. Genest, R. Hodges, W. Urbach, *Proc. Natl. Acad. Sci. USA* **2006**, *103*, 2098; b) A. Naji, A. J. Levine, P. A. Pincus, *Biophys. J.* **2007**, *93*, L49.

[12] a) C. H. Yu, J. B. Law, M. Suryana, H. Y. Low, M. P. Sheetz, *Proc Natl Acad Sci USA* **2011**, *108*, 20585; b) C. H. Yu, N. B. Rafiq, A. Krishnasamy, K. L. Hartman, G. E. Jones, A. D. Bershadsky, M. P. Sheetz, *Cell Rep.* **2013**, *5*, 1456; c) C. H. Yu, N. B. Rafiq, F. Cao, Y. Zhou, A. Krishnasamy, K. H. Biswas, A. Ravasio, Z. Chen, Y. H. Wang, K. Kawauchi, G. E. Jones, M. P. Sheetz, *Nat. Commun.* **2015**, *6*, 8672.

[13] Y. Wang, M. H. Kim, H. Shirahama, J. H. Lee, S. S. Ng, J. S. Glenn, N. J. Cho, *Sci. Rep.* **2016**, *6*, 37427.

[14] J. T. Groves, R. Parthasarathy, M. B. Forstner, *Annu. Rev. Biomed. Eng.* **2008**, *10*, 311.
[15] a) J. T. Groves, L. K. Mahal, C. R. Bertozzi, *Langmuir* **2001**, *17*, 5129; b) A. S. Andersson, K. Glasmästar, D. Sutherland, U. Lidberg, B. Kasemo, *J. Biomed. Mater. Res., Part A* **2003**, *64*, 622; c) L. Kam, S. G. Boxer, *J. Biomed. Mater. Res.* **2001**, *55*, 487.
[16] a) F. Li, S. D. Redick, H. P. Erickson, V. T. Moy, *Biophys. J.* **2003**, *84*, 1252; b) M. Morimatsu, A. H. Mekhdjian, A. S. Adhikari, A. R. Dunn, *Nano Lett.* **2013**, *13*, 3985.
[17] a) W. J. Parak, R. Boudreau, M. Le Gros, D. Gerion, D. Zanchet, C. M. Micheel, S. C. Williams, A. P. Alivisatos, C. Larabell, *Adv. Mater.* **2002**, *14*, 882; b) T. Pellegrino, W. J. Parak, R. Boudreau, D. Gerion, A. P. Alivisatos, C. A. Larabell, *Differentiation* **2003**, *71*, 542; c) T. Pellegrino, S. Kudera, T. Liedl, A. Muñoz Javier, L. Manna, W. J. Parak, *Small* **2005**, *1*, 48.
[18] a) A. S. Klein, M. Schaefer, T. Korte, A. Herrmann, A. Tannert, *Exp. Cell Res.* **2012**, *318*, 809; b) M. Shinitzky, M. Inbar, *J. Mol. Biol.* **1974**, *85*, 603; c) A. Chabanel, M. Flamm, K. Sung, M. Lee, D. Schachter, S. Chien, *Biophys. J.* **1983**, *44*, 171.
[19] J. S. Goodwin, K. R. Drake, C. L. Remmert, A. K. Kenworthy, *Biophys. J.* **2005**, *89*, 1398.
[20] a) P. K. Ghosh, A. Vasanji, G. Murugesan, S. J. Eppell, L. M. Graham, P. L. Fox, *Nat. Cell Biol.* **2002**, *4*, 894; b) A. Vasanji, P. K. Ghosh, L. M. Graham, S. J. Eppell, P. L. Fox, *Dev. Cell* **2004**, *6*, 29.
[21] S. R. Tabaei, J. A. Jackman, S.-O. Kim, B. Liedberg, W. Knoll, A. N. Parikh, N.-J. Cho, *Langmuir* **2014**, *30*, 13345.
[22] a) E. Evans, E. Sackmann, *J. Fluid Mech.* **1988**, *194*, 553; b) S. R. Tabaei, J. J. Gillissen, N. J. Cho, *Small* **2016**, *12*, 6338.
[23] B. Sanii, A. N. Parikh, *Soft Matter* **2007**, *3*, 974.
[24] C. Keller, B. Kasemo, *Biophys. J.* **1998**, *75*, 1397.
[25] R. Merkel, E. Sackmann, E. Evans, *J. Phys.* **1989**, *50*, 1535.
[26] P. Jönsson, J. P. Beech, J. O. Tegenfeldt, F. Höök, *Langmuir* **2009**, *25*, 6279.